Hindawi
International Journal of Distributed Sensor Networks
Volume 2024, Article ID 4022298, 14 pages
https://doi.org/10.1155/2024/4022298

Research Article

VCH: A Velocity Measurement Method Combining HFM Signals

Wei Yan,[1] Caixia Song,[2] Yuankun Peng,[1] and Zeng Liang[1,3]

[1]*Hangzhou Institute of Applied Acoustics, Hangzhou 310023, China*
[2]*College of Science and Information, Qingdao Agricultural University, Qingdao 266109, China*
[3]*Eastern Communication Company Limited, Hangzhou 310023, China*

Correspondence should be addressed to Yuankun Peng; pykqa2020@163.com

Received 16 May 2023; Revised 21 February 2024; Accepted 7 March 2024; Published 4 April 2024

Academic Editor: Yuedong Xie

During sonar detection, the fuzzy function of hyperbolic frequency modulation (HFM) in the waveform of active signal is in the shape of a "oblique blade," which leads to the coupling characteristics of its fuzzy function in the time dimension and frequency dimension. Doppler causes a frequency shift in the frequency dimension and a time delay in the time dimension, which makes it impossible for a single HFM signal to measure speed accurately. However, the time delay caused by the same moving target to HFM signals with different frequency bands and different pulse widths is also different. A velocity measurement method combining HFM signals (VCH) is proposed, which employs the time delay correlation between the combined HFM signals to achieve the target distance and speed. In the VCH method, the echo signal is no longer matched and filtered as a whole but is divided into two channels and matched and filtered separately. And then, the combined HFM signals are used to obtain the distance and speed of the target. Extensive simulation results show that the proposed method can estimate the distance and speed of moving targets accurately, and it has reference value for engineering application.

1. Introduction

As the level of submarine shock absorption and noise reduction is getting higher and higher, the noise source level of target radiation is getting smaller and smaller. Therefore, it is difficult to find the target using passive detection, and active detection becomes more and more important. By sending a signal and then analyzing and processing the received waveform, called signal processing, active detection can obtain part of the information of the target. However, during the transmission process, the acoustic information is affected by the medium and disturbed by the background, and thus, the obtained information is vague and uncertain. Moreover, the analysis of the characteristics of the received waveform can eliminate the nontarget information interference, and the selection of the transmitted waveform can reduce the influence of the medium, such as multichannel. A sonar system with excellent performance can obtain the target signal reliably in the shortest time. To achieve this goal, a good choice of transmit waveforms and receiver signal processing are two fundamental factors (Zhu [1], Qiao et al. [2], Bilal et al. [3]). Commonly used signal forms include pulsed continuous wave (PCW) or called as continuous wave (CW), linear frequency modulation (LFM), and hyperbolic frequency modulation (HFM).

Fixed targets have no velocity, and seamounts and fixed objects on the bottom of the sea greatly interfere with the detection and target determination. Therefore, the main issue to be solved in this paper is to use speed measurement to exclude the interference of fixed targets and calculate the speed and distance of moving targets at the same time. Velocity can be used to measure the motion characteristics of the target (Essa et al. [4], Bergies et al. [5]) and can be used as a factor of Kalman filter tracking to form a stable tracking trajectory (Elsisi et al. [6], Elsisi et al. [7]). Measuring the velocity of a target to the ground is an important basis for judging the existence of an underwater target. However, the movement of the target will cause the Doppler effect of the echo. And based on this, the speed of the moving target can be calculated by Doppler.

For PCW signal, the marine environment is a complex filter, which is a time-varying and space-varying channel,

in which signals propagate and cause distortion of signal waveform or spectrum. The single PCW signal propagating in the channel is easy to be filtered out in the ocean channel, and the effectiveness of speed measurement is thus limited. Shao et al. [8] employ HFM+PCW-combined signal as detection signal, to achieve multiparameter joint estimation of the azimuth-range speed of underwater moving point targets, in which the HFM signal is used for distance measurement and the PCW signal is used for speed measurement. Due to the unstable characteristics of the PCW signal in the sound field, it cannot continuously and effectively contact the target. When the signal-to-noise ratio (SNR) slightly does not meet the requirements, it will cause large speed measurement errors or even a wrong speed.

The LFM signal has a certain bandwidth and can overcome the shortcomings of single-frequency signals. However, single LFM has the following disadvantages (Zhang [9]):

(1) For the target whose distance and speed are unknown, LFM can only correctly determine the joint value of speed and distance. The joint value is the inclined axis in the fuzzy graph, and the distance and velocity cannot be known exactly

(2) For multiple targets with relative distances and relative velocities located near the inclined axis, LFM cannot resolve them

Although LFM signal has the above disadvantages, in fact, LFM signal is the most commonly used signal form of pulse compression radar currently. This is because the above shortcomings are the case of single pulse echo, but in fact, the radar observation target has more than one pulse in a short time, and the relationship between pulses can be used to overcome the above shortcomings. On the other hand, in sonar, the speed of sound in water is only 1500 m/s, which is not the same order of magnitude as the speed of electromagnetic waves in air radar, which is 3×10^8 m/s, and there is only one pulse echo in a short time. The LFM has a certain tolerance of Doppler. When LFM bandwidth is narrow and target speed is too large, Doppler mismatch is easy to be caused. Thus, the detection performance is reduced. Zhang et al. [10] proposed the use of combined LFM signals for accurate velocity measurement. This method overcomes the shortcomings of a single LFM, but it does not point out any method for velocity solution. At the same time, the method has particularly high requirements for the SNR. When the SNR is too low and the LFM has no peak output, it causes the result to fail.

The hyperbolic frequency modulation (HFM) signal and the LFM signal have the same advantages as above. Moreover, the HFM signal is not sensitive to Doppler (Tian et al. [11]). The Doppler motion will cause the peak of HFM-matched filter to move on the time axis. The higher the target velocity is, the more the peak value moves, but the amplitude of the peak value is not affected by Doppler. It is well known that sonar and radar echolocation systems learn from the echolocation systems of creatures such as bats and dolphins, whose ultrasonic signals have the same waveform structure. And their transmitted signals are all HFM signals. From an evolutionary point of view, HFM signal has an advantage in target range velocity estimation (Pang et al. [12]). HFM is widely used as a preamble signal in underwater acoustic communications (Liu and Song [13], Zhou and Wang [14]). The ambiguity function of an HFM has a tilted slowly decaying ridge, which can mitigate range-rate-caused detection degradation (Song et al. [15]). Peng et al. [16] used HFM and LFM signals with the same frequency band and the same pulse width for speed measurement. This method takes advantage of the advantages of HFM and LFM at the same time, but it needs to meet certain requirements for SNR. When the SNR is too low, LFM has no peak output, resulting in failure of distance and speed calculation. Therefore, the method used in this paper is introduced and derived based on HFM signals.

In this paper, a velocity measurement method combining HFM signals (VCH) is proposed, which employs the time delay correlation between the combined HFM signals to solve the target distance and speed. In the VCH method, the idle interval T is introduced between the combined signals, and thus, the original signal processing method is changed. Moreover, in the VCH method, the echo signal is no longer matched and filtered as a whole but is divided into two channels and matched and filtered separately. And then, the combined signals are used to obtain the distance and speed of the settlement target at the peak point. On the other hand, in the VCH method, the combined HFM signals are introduced into the detection. Due to the instability effect of PCW signal in the channel, its speed measurement effectiveness is limited. The HFM signal has a certain bandwidth. Even if the loss of a certain frequency point is too large, other frequency points are still returned by the echo energy, which can overcome the limitation of the unstable effect of single frequency. In this paper, the influence of moving target on delay and pulse width caused by HFM-combined signals can be used to measure speed and distance, which can improve the accuracy of measuring speed and distance. The main contributions of this paper are threefold:

(1) The combined HFM signals are introduced into the detection signal to overcome the shortcomings of a single HFM, and the combined HFM pulse signals can be flexibly configured

(2) The blank interval is introduced into the combined HFM signals to resist multipath delay and Doppler delay

(3) The combined HFM signals have a certain bandwidth, which can overcome the instability of single frequency (only one frequency point)

The rest of this paper is organized as follows: Section 2 reviews the related works. Section 3 describes the proposed VCH method in detail. Section 4 first introduces the key factor used in the formula derivation: the range-Doppler coupling characteristic of combined HFM signals, so as to derive the velocity and ranging of combined HFM signals. Simulation evaluation is given in Section 5. Finally, Section 6 concludes this paper.

2. Related Works

For the sonar velocity measurement problem, many scholars are currently conducting research. According to the change of the frequency of the HFM signal echo by the moving target, a tolerant matched filter is proposed (Murray [17]). However, the paper only points out the frequency of the HFM signal echo and fails to effectively use it to calculate the ranging delay caused by Doppler. In Xin [18], an improved preamble waveform UMD-HFM is proposed. On the basis of the UD-HFM signal, a blank interval is added to resist the delay expansion and Doppler delay of the multipath channel to avoid waveform stacking is shown, but the use and variation of blanking intervals are not indicated. Peng et al. [16] used HFM and LFM signals with the same frequency band and the same pulse width for speed measurement. This method takes advantage of the advantages of HFM and LFM at the same time, but it needs to meet certain requirements for SNR. When the SNR is too low, LFM has no peak output, resulting in failure of distance and speed calculation. Based on the Doppler invariant characteristics and pulse compression characteristics of HFM signal and the characteristics of Doppler sensitivity of continuous wave (CW) signal, Shao et al. [8] employ HFM+CW-combined signal as detection signal, to achieve multiparameter joint estimation of the azimuth-range speed of underwater moving point targets. The matching filtering method and waveform tracking method cannot always maintain the best speed estimation performance. To solve this problem, an improved Doppler sonar velocity estimation method based on accuracy evaluation and selection is proposed (Yang and Fang [19]). The Doppler sonar echo is divided into segments of the same width as the emitted pulse, and each segment is treated as an echo corresponding to the water layer. According to the results, the velocity estimation accuracy of each segment is positively correlated with the ratio of its autocorrelation module to its power. Zhang et al. [10] proposed the use of combined LFM signals for accurate velocity measurement. This method overcomes the shortcomings of a single LFM, but it does not point out any method for velocity solution. Compared with LFM signals, HFM signals have good pulse compression performance and Doppler invariance and are widely used in scenarios with serious Doppler effects such as radar reconnaissance and underwater acoustic detection (MA et al. [20]). Therefore, the parameter estimation problem of HFM signal is particularly important. A fast algorithm for HFM signal parameter estimation based on likelihood function is proposed. Firstly, the Cramer-Rao lower bound of the HFM signal as the performance evaluation standard for parameter estimation is reduced. Secondly, the likelihood function of the HFM signal based on Gaussian random noise is constructed, and an improved fitness function combined with the characteristics of data vectorization is proposed. Finally, the global optimal guided artificial bee colony (GABC) algorithm is used to optimize the fitness function to achieve the parameter estimation of the HFM signal. Liu et al. [21] pointed out that the Doppler motion is used to measure the speed and distance of the positive and negative HFM signals in opposite directions and proportional in size. But this method has a limitation; that is, the combined HFMs are required to have the same pulse width and the same frequency band. This requirement severely limits the flexibility of use. After that, Liu and Song [13] used a combined hyperbolic FM signal for speed measurement to overcome the above shortcomings and used two combined HFMs for distance measurement and speed measurement, but the default is that the two signals are emitted next to each other in time, and matched filtering is also two signals. Immediately after processing them together, Liu et al. pointed out in the article that the combined hyperbolic FM signal is used for speed measurement, but in actual engineering, it is difficult to realize in engineering due to the characteristics of transducer and transmitter.

3. HFM Signal Processing Steps in the VCH Method

In the VCH method, signal processing process is divided into two steps: HFM signal transmission (signal generation) and matched filtering of echo (pulse compression).

3.1. HFM Signal Transmission (Signal Generation). Design the signal, and decide whether to access the time interval T_s according to actual needs. Since the ocean channel is a time-varying and space-varying signal channel, various factors should be comprehensively considered to determine the transmission frequency band and pulse width of the combined signal. On the one hand, if the signal pulse width T is too short, only a small signal processing gain (10 log (T)) can be obtained. On the other hand, if the signal pulse width T is too long, the head and tail of the signal will be irrelevant, making part of the transmitted signal useless. The signal generation process is as shown in Figure 1.

3.2. Matched Filtering of Echo (Pulse Compression). Let $S(j\omega)$ and $s_o(t)$ denote the Fourier transform of $s(t)$ and the output signal after the Fourier transform of $s(t)$, respectively. And we have

$$s_o(t) = \frac{1}{2\pi}\int_{-\infty}^{+\infty} H(j\omega)S(j\omega)e^{j\omega t}d\omega. \tag{1}$$

At time t_m, the output signal $s_o(t_m)$ after the Fourier transform of $s(t)$ can be calculated as

$$s_o(t_m) = \frac{1}{2\pi}\int_{-\infty}^{+\infty} H(j\omega)S(j\omega)e^{j\omega t_m}d\omega. \tag{2}$$

Let $n(t)$ represent the white noise, and its power spectrum is constant N. Then, the power spectrum of the output noise $n_0(t)$ is $|H(j\omega)| \times N$. $n_o^2(\mathrm{t})$ can be calculated as

$$n_o^2(\mathrm{t}) = \frac{N}{2\pi}\int_{-\infty}^{+\infty} |H(j\omega)|^2 d\omega. \tag{3}$$

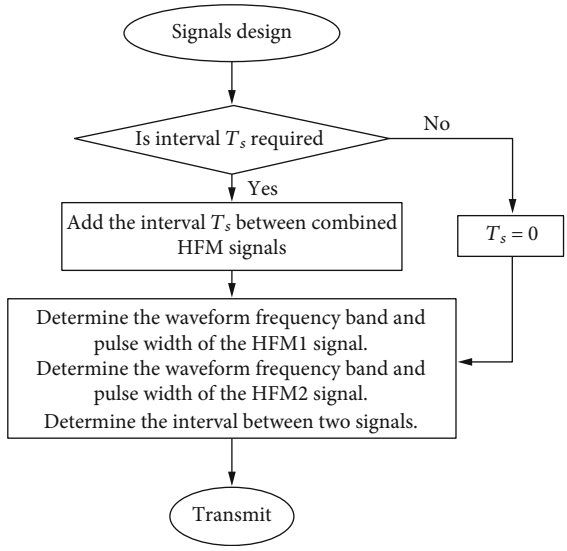

Figure 1: The generation process of the combined HFM signals.

And then, the SNR ρ can be calculated as

$$\rho = \frac{s_o^2(t)}{n_o^2(t)} = \frac{\left|\int_{-\infty}^{+\infty} H(j\omega)S(j\omega)e^{j\omega t}d\omega\right|^2}{2\pi N\int_{-\infty}^{+\infty}|H(j\omega)|^2 d\omega}. \tag{4}$$

According to the Cauchy-Schwartz inequality, Equation (5) satisfies the conditions of the equation and can be expressed as Equation (6).

$$\left|\int_{-\infty}^{+\infty} H(j\omega)S(j\omega)e^{j\omega t}d\omega\right|^2 \le \int_{-\infty}^{+\infty}|H(j\omega)|^2 d\omega\int_{-\infty}^{+\infty}|S(j\omega)|^2 d\omega, \tag{5}$$

$$H(j\omega) = k\left[S(j\omega)e^{j\omega t_m}\right]^*. \tag{6}$$

Then, Equation (4) can be replaced by

$$\rho = \frac{s_o^2(t)}{n_o^2(t)} \le \frac{1}{2\pi N}\int_{-\infty}^{+\infty}|S(j\omega)|^2 d\omega. \tag{7}$$

Then, the maximum output value $\rho_{\max}$ of the filter terminal is

$$\rho_{\max} = \frac{1}{2\pi N}\int_{-\infty}^{+\infty}|S(j\omega)|^2 d\omega. \tag{8}$$

Equation (6) needs to satisfy the condition that

$$H(j\omega) = kS(-j\omega)e^{-j\omega t_m}. \tag{9}$$

Due to the amplitude-frequency characteristic of the filter's transfer function, that is, $|H(j\omega)| = |S(-j\omega)|$, the filter in the frequency domain whose signal spectrum power (equal to 0) is completely cut off, so that the noise spectrum power in these regions cannot pass through. On the other hand, in the frequency domain where signal and noise coexist, the higher the signal spectrum power is, the more unobstructed the frequency domain is, and the lower the power is, the more blocked the frequency domain is. When detecting a signal in a known frequency band, since the spectral amplitude of the noise is uniform, such a filter can be designed to suppress the noise energy as much as possible (only the noise in the same frequency band as the signal can pass) and pass as much signal energy as possible.

The phase-frequency characteristics of the filter are $\psi_H = -\psi_s$. The original signal has a nonlinear phase-frequency change, so the highest points of the amplitudes of each frequency are staggered from each other and cannot be superimposed at the same time. On the other hand, after the correction of the phase-frequency characteristics of the filter, the phase of the output signal spectrum is 0, which makes the highest amplitude point of all frequency components achieve in-phase superposition at the output point. And a very narrow peak point output can thus be obtained.

The signal processing complexity of beamforming remains unchanged. The matched filtering method is different from the previous overall matched filtering. The echo signal is divided into two channels for separate matched filtering. Compared with the conventional processing, double the complexity of the signal processing, and the time complexity is $O(2)$. The processing flow chart is shown in Figure 2. According to the peak arrival time (t_1, t_2) of the corresponding positions, the distance formula and the speed formula can be used to calculate the distance and the speed.

In this section, the signal processing process for the generation of HFM-combined signals (how to combine and transmit) and the subsequent processing of echoes (how to perform matched filtering) are presented. In the next section, how to use the peak arrival time of the combined signal (t_1, t_2) to calculate the distance and speed of the target is given.

4. Derivation of Velocity and Ranging of Combined HFM Signals

In order to obtain the velocity and distance measurement formula of the combined signal, the key factor used in the formula derivation is introduced first: the range-Doppler coupling characteristic of combined HFM signals.

4.1. HFM Signal Delay. Let $s(t)$ represent the function expression of the waveform of HFM signal over time, f_1 represent the start frequency of the HFM signal, f_2 represent the stop frequency of the HFM signal, and T represent the pulse width of the HFM signal. We have

$$s(t) = \exp\left(j\times\frac{2\pi}{b}\ln\left(1+bf_1t\right)\right), \quad 0\le t\le T, \tag{10}$$

where $b = (f_1 - f_2)/(f_1 f_2 T)$.

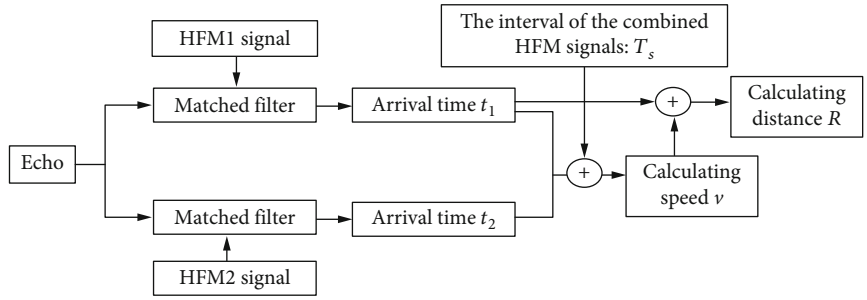

Figure 2: Echo-matched filtering process.

Deriving the instantaneous phase of HFM to obtain its instantaneous frequency $f_s(t)$, we have

$$f_s(t) = \frac{f_1}{1 + bf_1 t}. \tag{11}$$

Let $s_r(t)$ represent the waveform time domain of the echo of the HFM signal, and we have

$$s_r(t) = \exp\left(j \times \frac{2\pi}{b} \ln\left(1 + bf_1 \eta t\right)\right), \tag{12}$$

where $\eta = (c + v)/(c - v)$, c denotes the speed of sound in water and $c = 1500$ m/s, and v denotes the speed of the target.

The Doppler change of the signal results in a change in the frequency of the echo $f_r(t)$ (Xin [18]), and we have

$$f_r(t) = \frac{\eta f_1}{1 + bf_1 \eta t}. \tag{13}$$

Since the HFM signal is not sensitive to Doppler, the HFM signal has the characteristics of Doppler invariance. Therefore, the change law of the instantaneous frequency $f_r(t)$ of the received signal does not change, and the instantaneous frequency of the original transmitted signal $f_s(t)$ is only shifted by a time Δt. We have

$$f_r(t) = f_s(t - \Delta t). \tag{14}$$

Based on Equation (13) and Equation (14), the Δt can be obtained.

$$\Delta t = \frac{f_1(1 - (1/\eta))T}{f_1 - f_0}. \tag{15}$$

Therefore, the HFM signal has the characteristics of Doppler invariance. When HFM signal is used to detect the target, the output amplitude of the sonar system does not change due to the relative motion between the target and the sonar. However, due to the additional time delay caused by Doppler in the HFM signal, the accuracy of the distance measurement will be reduced, as shown in Figure 3.

In this section, the distance Doppler coupling formula of a single HFM signal is derived, and the formula for calculating the matched filter delay Δt caused by the target Doppler is thus obtained, which provides technical support for the derivation of the next section. In the following section, the formula for distance measurement of combined HFM signals will be derived.

4.2. Velocity and Ranging of Combined HFM Signals. HFM1 signal: the starting frequency of the HFM1 signal is f_{10}, the ending frequency of the HFM1 signal is f_{11}, and the pulse width of HFM1 signal is T_1.

HFM2 signal: the starting frequency of the HFM1 signal is f_{20}, the ending frequency of the HFM1 signal is f_{21}, and the pulse width of HFM1 signal is T_2.

Now, we use the combined HFM signals to calculate the speed and distance of the target. Let t_1 and t_2 represent the peak output time of combined HFM1 signal and HFM2 signal, respectively.

$$t_1 = \frac{2R}{c} + \Delta t_1, \tag{16}$$

$$t_2 = \frac{2R}{c} + \Delta t_2 + \frac{T_1}{\eta} + \frac{T_s}{\eta}, \tag{17}$$

where $\Delta t_1 = (f_{11}T_1(1 - 1/\eta))/(f_{10} - f_{11})$ and $\Delta t_2 = (f_{21}T_2(1 - (1/\eta)))/(f_{20} - f_{21})$

And then, we have

$$\Delta t_1 - \Delta t_2 = \left(1 - \frac{1}{\eta}\right)\left(\frac{f_{11}T_1}{f_{10} - f_{11}} - \frac{f_{21}T_2}{f_{20} - f_{21}}\right) = \left(1 - \frac{1}{\eta}\right)A, \tag{18}$$

where $A = (f_{11}T_1/(f_{10} - f_{11})) - (f_{21}T_2/(f_{20} - f_{21}))$.

Based on Equation (16) and Equation (17), we have

$$t_1 - t_2 = \Delta t_1 - \Delta t_2 - \frac{1}{\eta}(T_1 + T_s). \tag{19}$$

The v can be derived as

$$v = \frac{B - 1}{B + 1}c, \tag{20}$$

where $B = (-T_1 - T_s - A)/(t_1 - t_2 - A)$

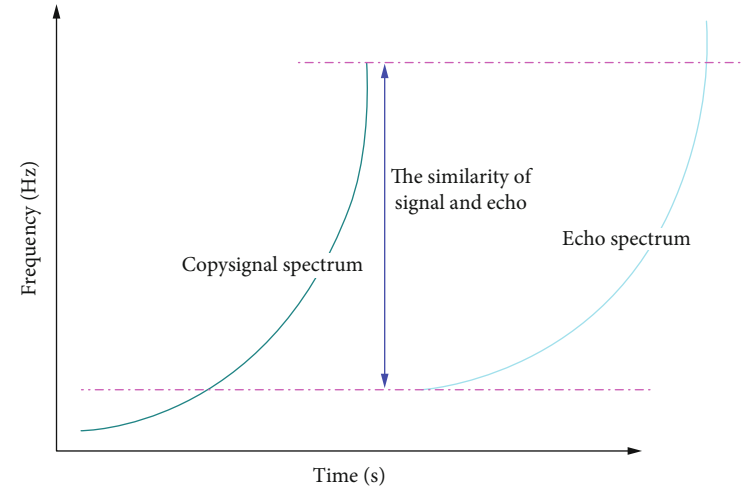

(a) Positive frequency modulation of HFM signal

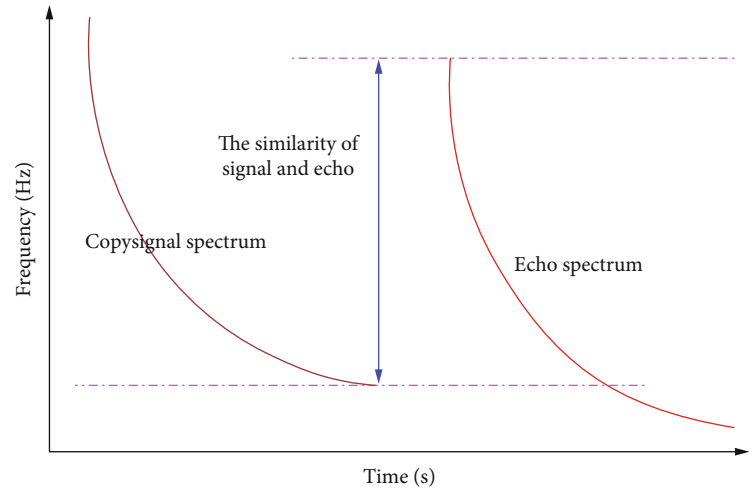

(b) Negative frequency modulation of HFM signal

Figure 3: Transformation of instantaneous frequency of HFM signal in Doppler.

Let R denote the distance between the sonar and the target, and we have

$$R = \frac{c}{2}\left(t_1 - \frac{f_{11}T_1}{f_{10} - f_{11}}\left(1 - \frac{c - ((B-1)/(B+1))c}{c + ((B-1)/(B+1))c}\right)\right). \quad (21)$$

When the HFM1 signal and HFM2 signal are the same, that is, $f_{20} = f_{10}$ and $f_{21} = f_{11}$. In this case, $A = 0$, that is, $B = (-T_1 - T_s)/(t_1 - t_2)$.

When the signal is a combination of positive and negative frequencies, that is, $A = (f_{11}T/(f_{10} - f_{11})) - (f_{11}T/(f_{10} - f_{11}))$.

In this section, the formula of distance measurement of combined HFM signals is derived. When the peak arrival time of the combined HFM signals is known, the distance and speed of the target can be calculated.

5. Performance Analysis

5.1. Simulation Settings. We set up three simulation environments for experimental comparison: simulation environment 1, simulation environment 2, and simulation environment 3.

5.1.1. Simulation Environment 1. In the HFM1 signal, $f_{10} = 1000$ Hz, $f_{11} = 2000$ Hz, and $T_1 = 3$ s. In the HFM2 signal, $f_{20} = 100$ Hz, $f_{21} = 300$ Hz, and $T_2 = 4$ s. For both HFM signals, the sample frequency is 6000 Hz. The signal interval between HFM1 and HFM2 is $T_s = 3$ s. The distance of the target from the sound source is 15 km. The SNR in the echo signal is -20 dB.

5.1.2. Simulation Environment 2. In the HFM1 signal, $f_{10} = 1000$ Hz, $f_{11} = 900$ Hz, and $T_1 = 3$ s. In the HFM2 signal, $f_{20} = 900$ Hz, $f_{21} = 1000$ Hz, and $T_2 = 4$ s. For both HFM signals, the sample frequency is 6000 Hz. The signal interval between HFM1 and HFM2 is $T_s = 0$ s. The distance of the target from the sound source is 15 km. The SNR in the echo signal is -20 dB.

5.1.3. Simulation Environment 3. In the HFM1 signal, $f_{10} = 1000$ Hz, $f_{11} = 1100$ Hz, and $T_1 = 3$ s. In the HFM2 signal,

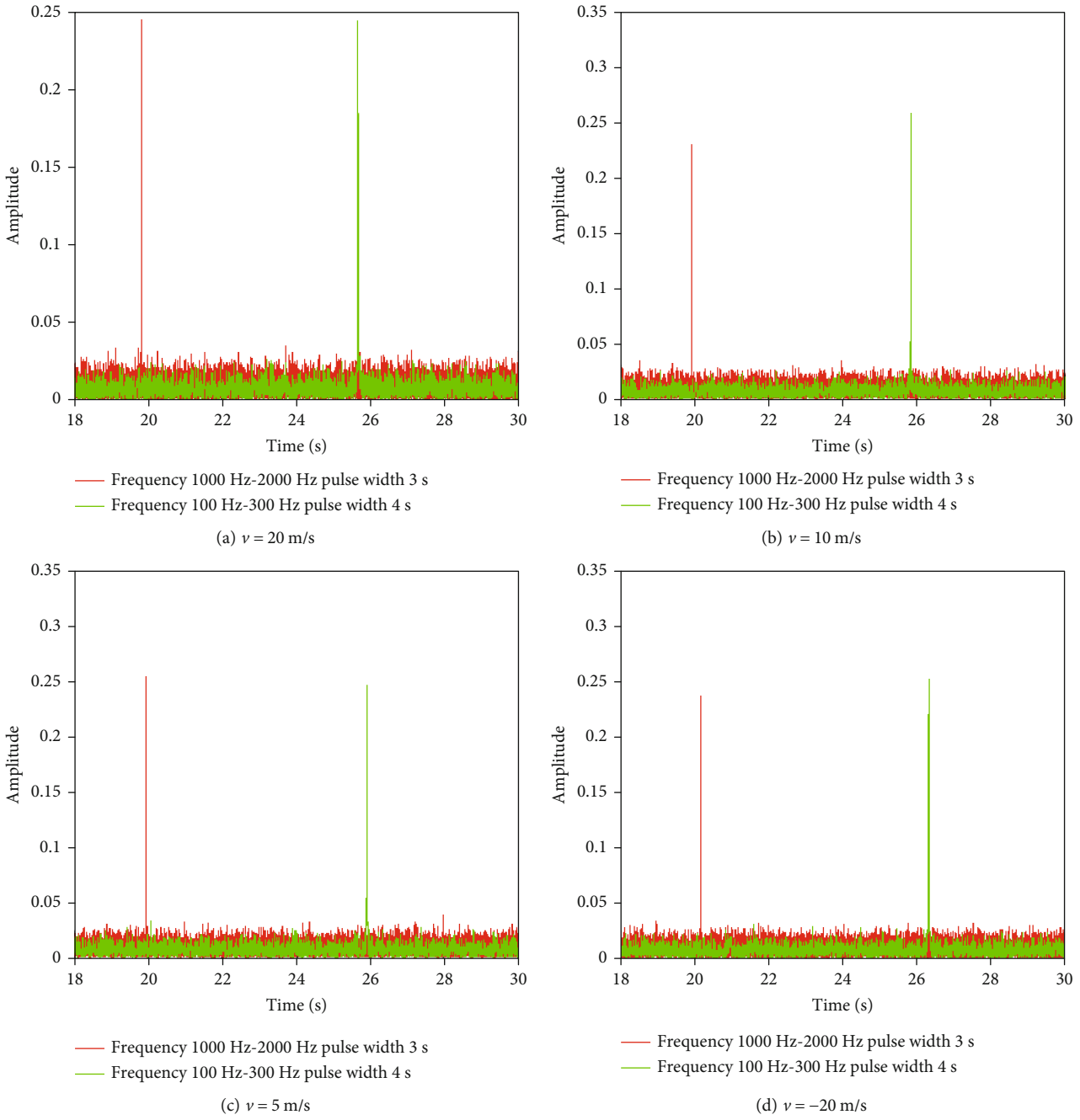

Figure 4: Continued.

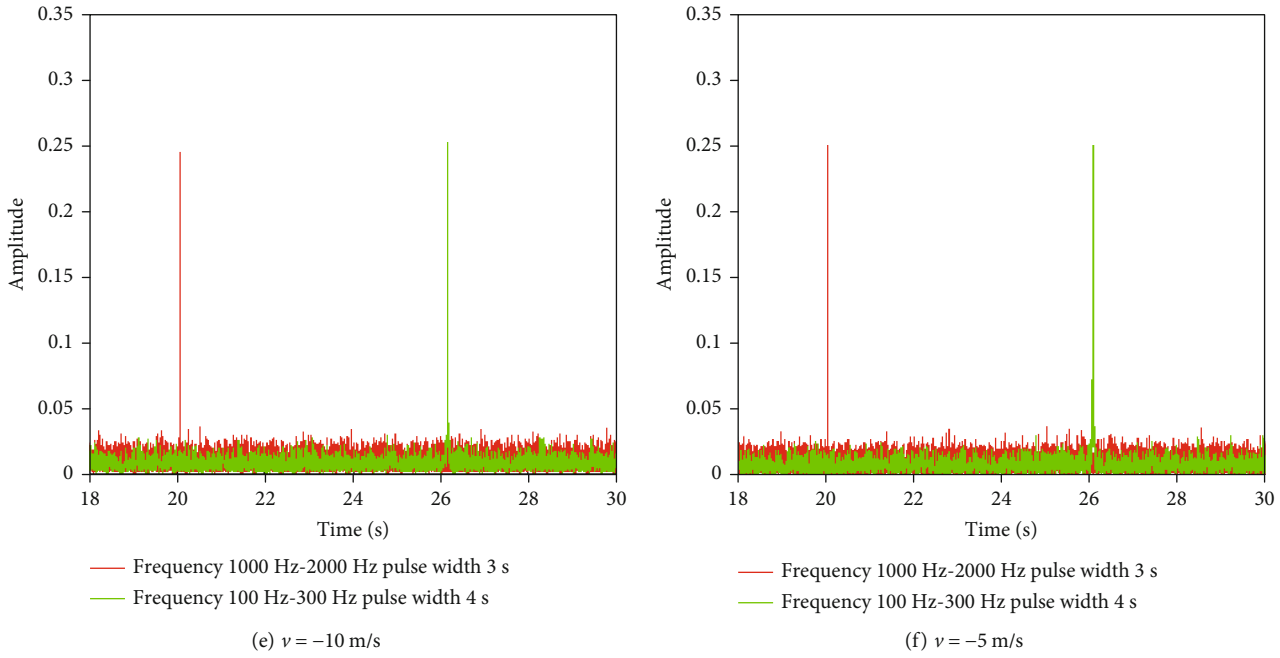

Figure 4: The output of matched filtering at various v under simulation environment 1.

Table 1: Results under simulation environment 1.

Speed (m/s)	Peak moment (s)		Speed measurement of VCH (m/s)	Ranging of VCH (km)	Speed measurement error of VCH	Ranging error of VCH	Ranging error of single signal		Range accuracy improvement ratio	
	t_1	t_2					HFM1	HFM2	Compared to HFM1	Compared to HFM2
20	19.8422	25.6843	19.9921	15	0.0395%	0%	0.789%	1.5785%	100%	100%
10	19.9205	25.8408	10.0249	15.0001	0.249%	0.000667%	0.3975%	0.796%	99.83229%	99.91625%
-5	19.9602	25.9202	5.0167	15.0001	0.334%	0.000667%	0.199%	0.399%	99.66499%	99.83292%
-20	20.1622	26.3242	-19.9803	15.0001	0.0985%	0.000667%	0.811%	1.621%	99.9178%	99.95887%
-10	20.0805	26.1608	-9.9749	15.0001	0.251%	0.000667%	0.4025%	0.804%	99.83437%	99.91708%
-5	20.0402	26.0803	-5.0041	15	0.082%	0%	0.201%	0.4015%	100%	100%

$f_{20} = 1000$ Hz, $f_{21} = 1100$ Hz, and $T_2 = 3$ s. For both HFM signals, the sample frequency is 6000 Hz. The signal interval between HFM1 and HFM2 is $T_s = 0$ s. The distance of the target from the sound source is 15 km. The SNR in the echo signal is -20 dB.

5.2. Simulation Results. Figure 4 shows the performance analysis under the simulation environment 1 at various v. Table 1 gives the numerical results of VCH. We take Figure 4(a) as an example to analyze the performance of VCH method under various speed v. From Figure 4(a), it can be seen that, after matched filtering, the combined signal echo time of HFM1 signal and HFM2 signal is 19.8422 s and 25.6843 s, respectively. According to Equation (20), the value of v is 19.9921 m/s. It can be seen from Table 1 that the speed measurement error and the ranging error of VCH are 0.0395% and 0%, respectively. The ranging error of single HFM1 signal and single HFM2 signal is 0.789% and 1.5785%, respectively. Compared with single HFM1 signal and single HFM2 signal, the ranging measurement accuracy of VCH is improved by 100% and 100%, respectively.

Figure 5 shows the performance analysis under the simulation environment 2 at various v. Table 2 gives the numerical results of VCH. We take Figure 5(a) as an example to analyze the performance of VCH method under various speed v. From Figure 5(a), it can be seen that, after matched filtering, the combined signal echo time of HFM1 signal and HFM2 signal is 20.7103 s and 22.1313 s, respectively. According to Equation (20), the value of v is 20.0007 m/s. It can be seen from Table 2 that the speed measurement error and the ranging error of VCH are 0.0035% and 0.001333%, respectively. The ranging error of single HFM1 signal and single HFM2 signal is 3.5515% and 19.3435%, respectively. Compared with single HFM1 signal and single HFM2 signal, the ranging measurement accuracy of VCH is improved by 99.96246% and 99.99311%, respectively.

Figure 6 shows the performance analysis under the simulation environment 3 at various v. Table 3 gives the

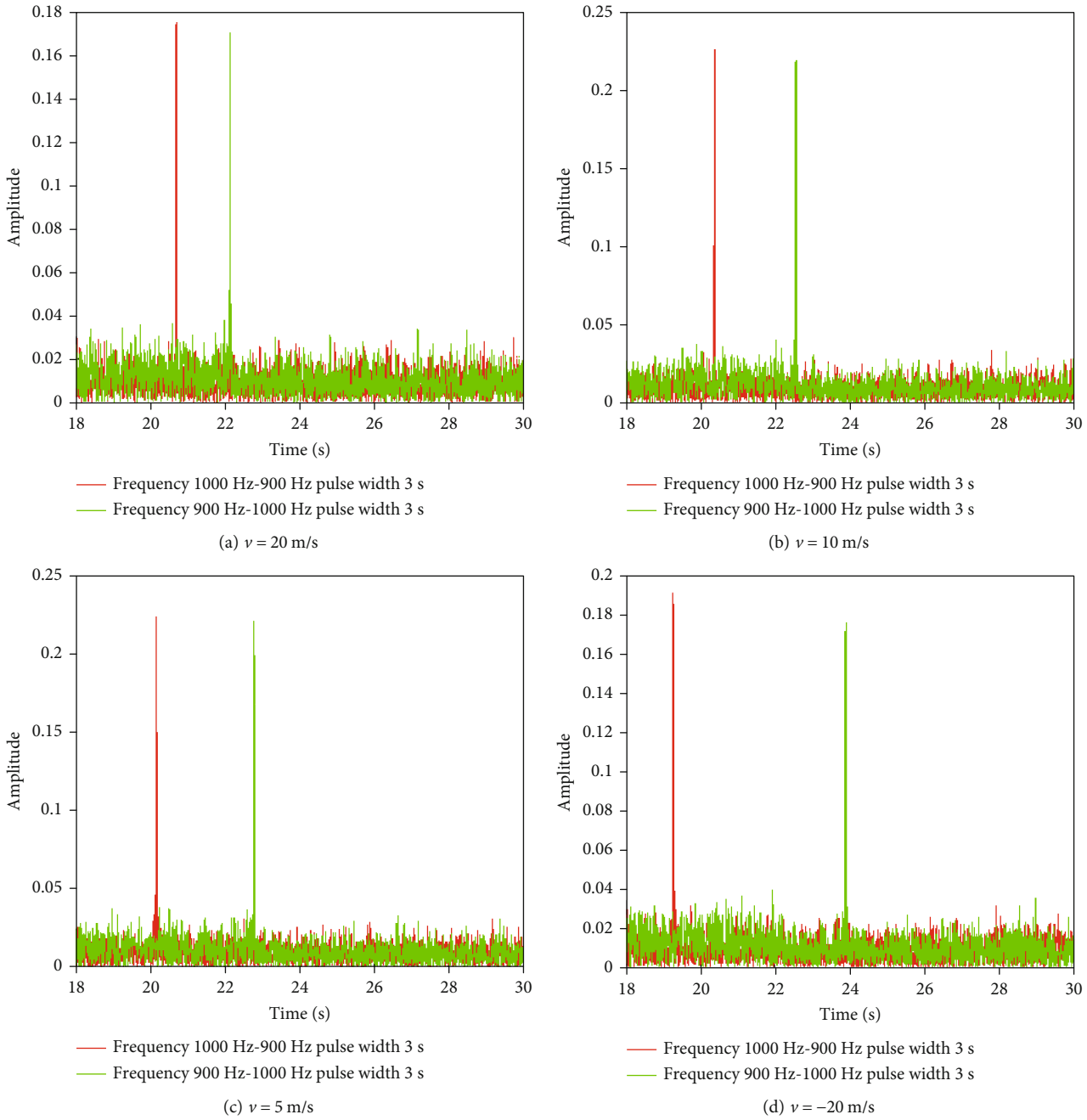

Figure 5: Continued.

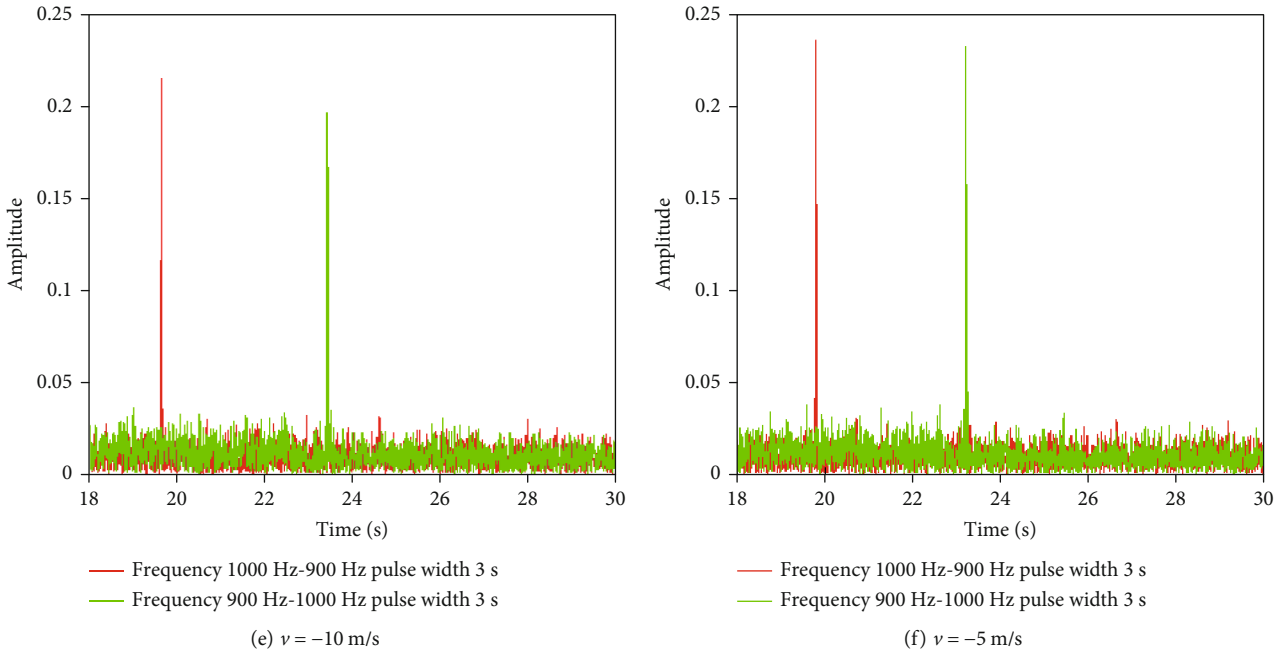

Figure 5: The output of matched filtering at various v under simulation environment 2.

Table 2: Results under simulation environment 2.

Speed (m/s)	Peak moment (s)		Speed measurement of VCH (m/s)	Ranging of VCH (km)	Speed measurement error of VCH	Ranging error of VCH	Ranging error of single signal		Range accuracy improvement ratio	
	t_1	t_2					HFM1	HFM2	Compared to HFM1	Compared to HFM2
20	20.7103	22.1313	20.0007	14.9998	0.0035%	0.001333%	3.5515%	19.3435%	99.96246%	99.99311%
10	20.3577	22.5625	10.0059	14.9998	0.059%	0.000667%	1.7885%	17.1875%	99.96272%	99.99612%
-5	20.1792	22.7807	4.9978	14.9998	0.044%	0.000667%	0.896%	16.0965%	99.9256%	99.99586%
-20	19.2698	23.8913	-19.9885	14.9996	0.0075%	0.002667%	3.651%	10.5435%	99.92696%	99.97471%
-10	19.6378	23.4425	-9.9913	15	0.087%	0%	1.811%	12.7875%	100%	100%
-5	19.8188	23.2207	-5.0062	14.9997	0.124%	0.002%	0.906%	13.8965%	99.77925%	99.98561%

numerical results of VCH. We take Figure 6(a) as an example to analyze the performance of VCH method under various speed v. From Figure 6(a), it can be seen that, after matched filtering, the combined signal echo time of HFM1 signal and HFM2 signal is 19.1313 s and 22.0517 s, respectively. According to Equation (20), the value of v is 20.1847 m/s. It can be seen from Table 3 that the speed measurement error and the ranging error of VCH are 0.9235% and 0.038667%, respectively. The ranging error of single HFM1 signal and single HFM2 signal is 4.3435% and 19.7415%, respectively. Compared with single HFM1 signal and single HFM2 signal, the ranging measurement accuracy of VCH is improved by 99.10978% and 99.80414%, respectively.

The above simulation environment includes both the same and the different HFM signals in the combination, both the same pulse width and different pulse width, and both the same modulation degree and the opposite modulation degree. According to Figures 4–6 and Tables 1–3, it can be seen that the speed and distance of the target can be accurately calculated. Compared to a single (separate) HFM signal, the combined HFM signals cannot only realize accurate speed measurement but also improve the accuracy of distance measurement.

At present, the commonly used velocity measurement method is continuous wave (CW) velocity measurement (Shao et al. [8]). Due to the instability of CW velocity measurement, the deviation of ranging velocity measurement occurs. A CW velocity measurement simulation is set up, as shown in Figure 7.

5.2.1. Simulation Environment 4. The sample frequency is 7000 Hz, the distance between the target and the source is 3.75 km, and the SNR of the echo signal is -10 dB. The frequency of CW is 1500 Hz, and pulse width is 3 s. It can be seen from Figure 7 that the target should appear at 5 s. Due to the influence of noise, the target appears at 5.9 s, and there is a deviation. The measurement effect is not as good as that of combined HFM signals under simulation environment 1. This is because the combined HFM signals

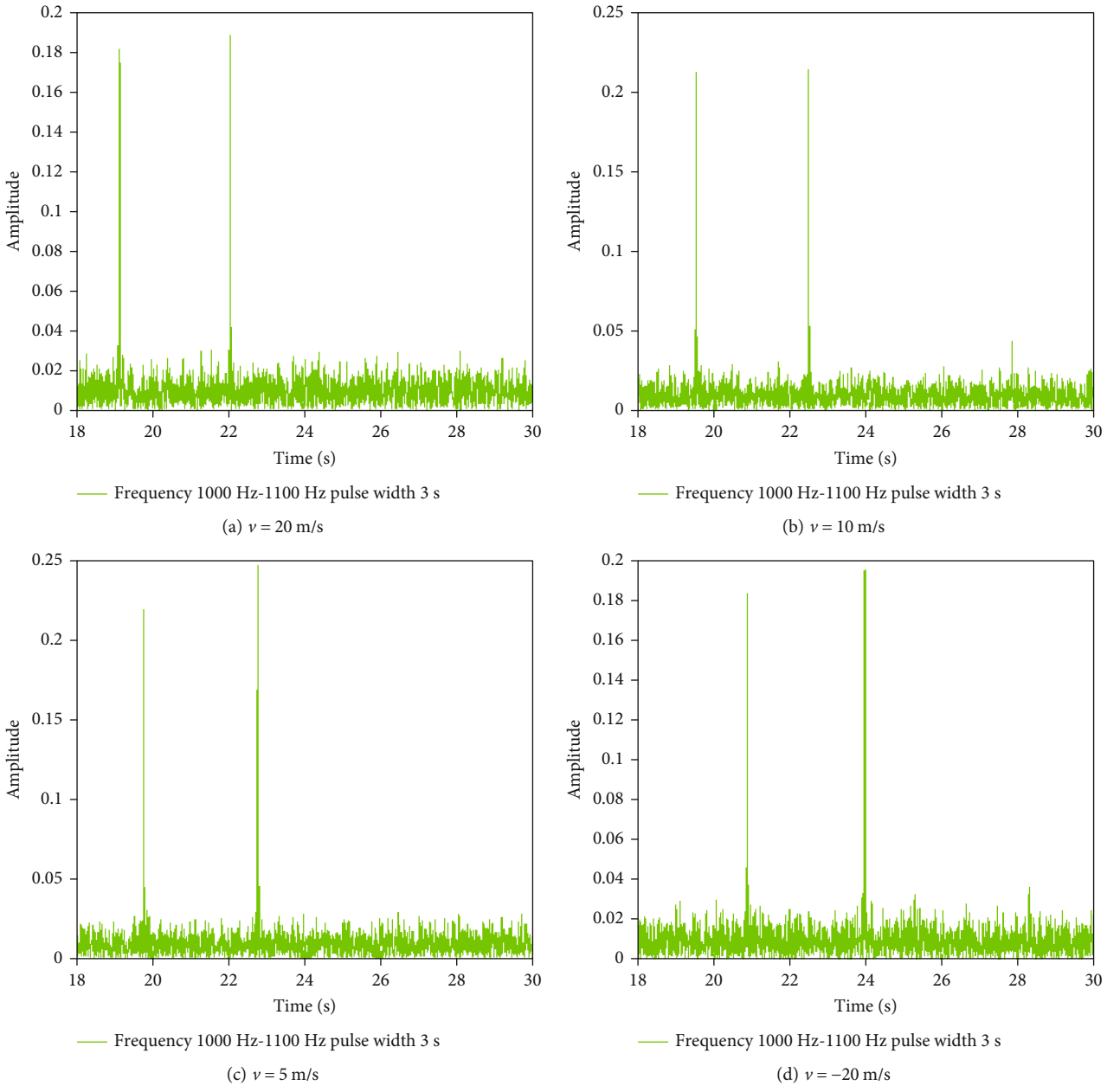

Figure 6: Continued.

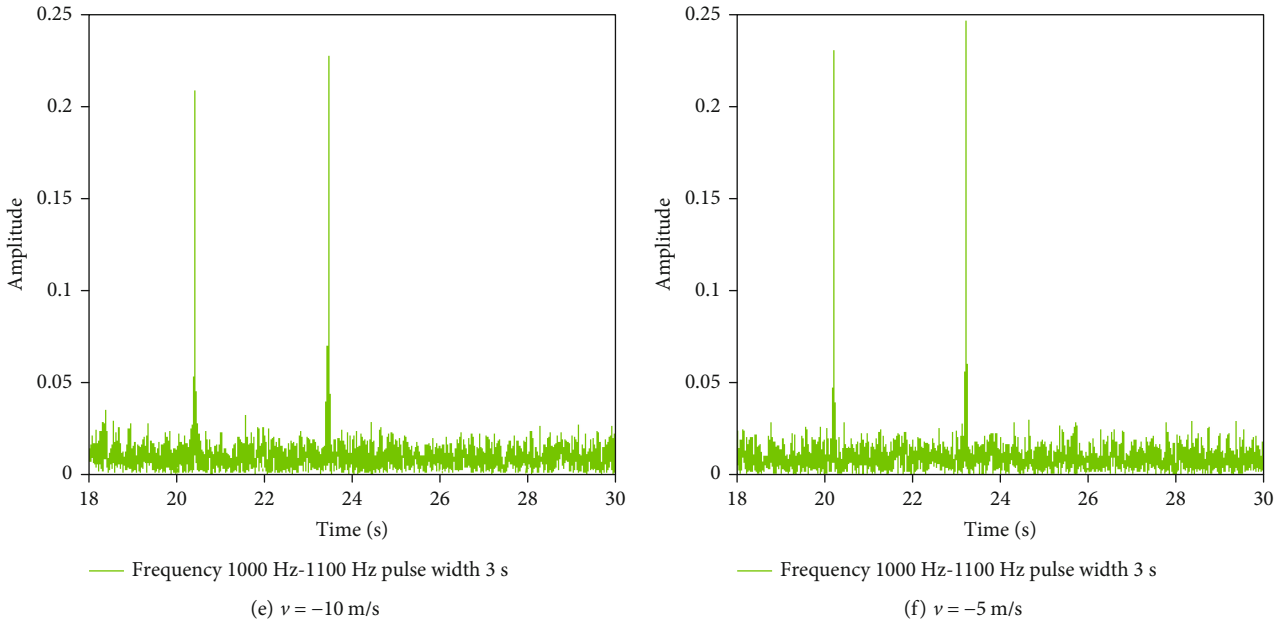

Figure 6: The output of matched filtering at various v under simulation environment 3.

Table 3: Results under simulation environment 3.

Speed (m/s)	Peak moment (s)		Speed measurement of VCH (m/s)	Ranging of VCH (km)	Speed measurement error of VCH	Ranging error of VCH	Ranging error of single signal		Range accuracy improvement ratio	
	t_1	t_2					HFM1	HFM2	Compared to HFM1	Compared to HFM2
20	19.1313	22.0517	20.1847	15.0058	0.9235%	0.038667%	4.3435%	19.7415%	99.10978%	99.80414%
10	19.563	22.523	10.0671	15.0022	0.671%	0.014667%	2.185%	17.385%	99.32876%	99.91564%
-5	19.7812	22.7607	5.1426	15.005	2.852%	0.033333%	1.094%	16.1965%	96.95308%	99.79419%
-20	20.8917	23.9732	-20.1019	14.9964	0.5095%	0.024%	4.4585%	10.134%	99.4617%	99.76317%
-10	20.443	23.4833	-10.016	14.9965	0.16%	0.003333%	2.215%	12.5835%	99.84951%	99.97351%
-5	20.2212	23.2405	-5	15.0064	0%	0.042667%	1.106%	13.7975%	96.14225%	99.69077%

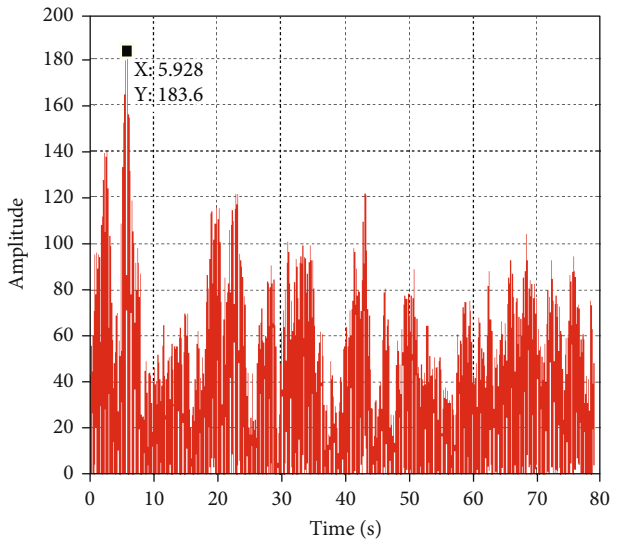

Figure 7: The output of matched filtering at various v under simulation environment 4.

can obtain more target information, which is more conducive to identification while measuring speed.

This section gives HFM forms of different combinations, all of which can realize the function of speed measurement, proving the feasibility of this method.

According to the above simulation results, it can be seen that the proposed VCH method can estimate the distance and speed of moving targets accurately, and these are mainly the following reasons: (1) a time interval is added in the VCH method. First, it is used to resist multipath delay expansion and Doppler delay to avoid superposition between waveforms. Second, considering the engineering realization of the transmitter, it is very difficult to realize the signal conversion engineering without interval. (2) The VCH method is no longer constrained by the signals in the combination. The frequency bands of the signals in the combination can be the same or different, and the frequency band and pulse width can be set independently. The modulation modes in the combined signal can be the same or different, such as positive and negative modulation, positive and negative modulation, and negative and negative

modulation. (3) When the signals in the combination are exactly the same, the Doppler is converted to the pulse width to solve the extraction.

6. Conclusion

The Doppler phenomenon of the same moving target has different delays for different signals in the combination, resulting in different arrival times of the signals in the combination, so the speed of the target can be solved by using the delay relationship of the signals in the combination. In this paper, a velocity measurement method combining HFM signals (VCH) is proposed, which employs the time delay correlation between the combined HFM signals to solve the target distance and speed. The delay caused by the movement of the target to the combined signal depends on the relationship between the frequency band and the pulse width of the combined signal. In order to fully obtain target information and provide sufficient information for subsequent target identification, the frequency bands of the combined signals should be separated (no overlapping or overlapping as little as possible). The pulse width requirements are not high and can be combined arbitrarily.

Through the Doppler effect of the moving target, the Doppler is transformed into the compression and frequency shift of the transmitted signal to form the Doppler echo. And the echo has a certain SNR. When the echo is too weak to stand out from the noise and the arrival time of the echo cannot be determined, then the algorithm fails. On the other hand, the marine environment is complex and changeable. In the process of detection, the echo of the combined signals may be too weak to detect due to excessive propagation loss at some time. In the future work, the combination of pulse train in multiple frequency bands can be used to solve above issue.

Data Availability

Access to data is restricted.

Conflicts of Interest

The authors declare that there is no conflict of interests regarding the publication of this paper.

Acknowledgments

This work was supported in part by the Shandong Smart Ocean Ranch Engineering Technology Collaborative Innovation Center, in part by the Shandong Agricultural Science and Technology Service Project (No. 2019FW037-4), in part by the Shandong Technology Innovation Guidance Program (No. 2020LYXZ023), in part by the Horizontal Project (No. 20193702010792), and in part by the Ministry of Education Industry-University Cooperation Collaborative Education Project (No. 201902005027, No. 201901029013, and No. 202101123035).

References

[1] K. Zhu, *Principle of active sonar detection information*, Science Press, 2014.

[2] G. Qiao, T. Ma, S. Liu, and M. Bilal, "A frequency hopping pattern inspired bionic underwater acoustic communication," *Physical Communication*, vol. 46, article 101288, 2021.

[3] M. Bilal, S. Liu, G. Qiao, L. Wan, and Y. Tao, "Bionic Morse coding mimicking humpback whale song for covert underwater communication," *Applied Sciences*, vol. 10, no. 1, p. 186, 2019.

[4] M. E. S. M. Essa, M. Elsisi, M. Saleh Elsayed, M. Fawzy Ahmed, and A. M. Elshafeey, "An improvement of model predictive for aircraft longitudinal flight control based on intelligent technique," *Mathematics*, vol. 10, no. 19, p. 3510, 2022.

[5] S. Bergies, S. F. Su, and M. Elsisi, "Model predictive paradigm with low computational burden based on dandelion optimizer for autonomous vehicle considering vision system uncertainty," *Mathematics*, vol. 10, no. 23, p. 4539, 2022.

[6] M. Elsisi, H. G. Zaini, K. Mahmoud, S. Bergies, and S. S. M. Ghoneim, "Improvement of trajectory tracking by robot manipulator based on a new co-operative optimization algorithm," *Mathematics*, vol. 9, no. 24, p. 3231, 2021.

[7] M. Elsisi, M. Altius, S. F. Su, and C. L. Su, "Robust Kalman filter for position estimation of automated guided vehicles under cyberattacks," *IEEE Transactions on Instrumentation and Measurement*, vol. 72, pp. 1–12, 2023.

[8] Z. Shao, T. Chen, and G. Wang, "A method of underwater moving target detection base on HFM and CW signals," in *2017 Western China Acoustics Academic Exchange Conference*, Hohhot, Inner Mongolia, China, 2017.

[9] Z. Zhang, *Radar Signal Selection and Processing*, National Defense Industry Press, 1979.

[10] B. Zhang, P. Liu, H. Zhao, Y. Peng, Z. Liang, and Y. Yang, "Research on LFM combined signal ranging method," in *2021 IEEE 4th International Conference on Electronic Information and Communication Technology (ICEICT)*, pp. 357–362, Xi'an, China, August 2021.

[11] T. Tian, G. Li, and D. Sun, *Sonar Technology*, Harbin Engineering University Press, 2nd edition, 2010.

[12] Y. Pang, Q. Yan, and S. Wang, "Research on hyperbolic frequency modulation signal speed measurement and ranging method," *Acoustics and Electrical Engineering*, vol. 4, no. 4, p. 4, 2014.

[13] P. Liu and C. Song, "Sch: a speed measurement method of combined hyperbolic frequency modulation signals," *IEEE Access*, vol. 9, pp. 95986–95993, 2021.

[14] S. Zhou and Z. Wang, *OFDM for underwater acoustic communications*, Wiley Publishing, 2014.

[15] X. Song, P. Willett, and S. Zhou, "Range bias modeling for hyperbolic-frequency-modulated waveforms in target tracking," *IEEE Journal of Oceanic Engineering*, vol. 37, no. 4, pp. 670–679, 2012.

[16] Y. Peng, C. Song, L. Qi et al., "JLHS: a joint linear frequency modulation and hyperbolic frequency modulation approach for speed measurement," *IEEE Access*, vol. 8, pp. 205316–205326, 2020.

[17] J. J. Murray, "On the Doppler bias of hyperbolic frequency modulation matched filter time of arrival estimates," *IEEE Journal of Oceanic Engineering*, vol. 44, no. 2, pp. 446–450, 2018.

[18] M. Xin, *HFM acoustic preamble signal detection algorithm based on match filter and waveform design in underwater communication*, PhD Thesis, Harbin Institute of Technology, 2017.

[19] Y. Yang and S. Fang, "Improved velocity estimation method for Doppler sonar based on accuracy evaluation and selection," *Journal of Marine Science and Engineering*, vol. 9, no. 6, p. 576, 2021.

[20] B. Ma, D. Yuan, and J. Liu, "Fast algorithm for parameter estimation of hyperbolic frequency modulation signals based on likelihood function," *Journal of Electronics and Information*, vol. 43, no. 5, pp. 1228–1234, 2021.

[21] P. Liu, H. Zhao, B. Zhang, B. Zhou, Y. Peng, and Y. Yang, "A positive and negative HFM for speed measurement," in *2021 IEEE 4th International Conference on Electronic Information and Communication Technology (ICEICT)*, pp. 352–356, Xi'an, China, August 2021.